Genetic Background Controls Tumor Development in *Pten*-Deficient Mice

Dan Freeman,[1] Ralf Lesche,[1] Nathalie Kertesz,[1] Shungyou Wang,[1] Gang Li,[1] Jing Gao,[1] Matthias Groszer,[1,2] Hilda Martinez-Diaz,[1] Nora Rozengurt,[2] George Thomas,[2] Xin Liu,[2] and Hong Wu[1]

Departments of [1]Molecular and Medical Pharmacology and [2]Pathology and Laboratory Medicine, University of California at Los Angeles School of Medicine, Los Angeles, California

Abstract

***PTEN* is one of the most frequently mutated tumor suppressor genes in human cancers. Germ line mutations of *PTEN* have been detected in three rare autosomal-dominant disorders. However, identical mutations in the *PTEN* gene may lead to different symptoms that have traditionally been described as different disorders, such as Cowden disease, Lhermitte-Duclos disease, and Bannayan-Zonana syndromes. This lack of genotype-phenotype correlation prompted us to directly test the possible effects of genetic background or modifier genes on PTEN-controlled tumorigenesis using genetically engineered mouse models. In this study, we generated two animal models in which either exon 5 (*Pten*$^{\Delta 5}$) or promoter to exon 3 (*Pten*$^{-}$) of the murine *Pten* gene were deleted and compared phenotypes associated with individual mutations on two genetic backgrounds. We found that the onset and spectrum of tumor formation depend significantly on the genetic background but less on the type of mutation generated. Our results suggest that PTEN plays a critical role in cancer development, and genetic background may influence the onset, the spectrum, and the progression of tumorigenesis caused by *Pten* mutation.** (Cancer Res 2006; 66(13): 6492-6)

Introduction

PTEN (phosphatase and tensin homologue deleted from chromosome 10) or *MMAC1* (mutated in multiple advanced cancers) is one of the most frequently mutated tumor suppressor genes in human cancers (1, 2). Germ line mutations of *PTEN* have been detected in three rare, autosomal-dominant disorders, Cowden disease, Lhermitte-Duclos disease, and Bannayan-Zonana syndrome (3, 4), which were originally identified as distinct syndromes. Although these disorders share similar pathologic features, such as benign tumors in multiple organs (hamartomas) and increased susceptibility to malignant cancers, the onset and spectrum of these clinical abnormalities are quite different. In some cases, patients with an identical mutation may have very different clinical symptoms and may be diagnosed with different diseases (5). Inactivation of *Pten* in mouse models, generated by three independent groups, has confirmed PTEN as a bona fide tumor suppressor (6–9). Although the targeted disruption centers on exon 5, which is known to contain the phosphatase domain, the three groups have subtle differences in excision ranging from exons 3 to 6 and consequently reported differences in the tumor spectra seen in mice. To clarify whether differences seen in both human patients and in animals models are due to (*a*) nature of individual mutations (e.g., hypomorphic variations in the *Pten* locus) or (*b*) genetic background/modifier genes, we generated two knockout mouse strains with different deletions and compared the consequences of *Pten* inactivation on 129/C57 and 129/BALB/c genetic backgrounds. Similar to previous reports, mice homozygous for both mutations die early during embryogenesis and mice with heterozygous *Pten* deletion develop tumors in various tissues. However, the onset and spectrum of tumor development shown in our study were quite different, and in particular, high incidence of prostate cancer and hemangioma formation was observed on 129/BALB/c background. Our study shows the crucial role of PTEN in prostate cancer formation and suggests that the genetic background or modifier gene(s) may have a significant effect on PTEN's biological functions.

Materials and Methods

Generation of *Pten*$^{+/-}$ and *Pten*$^{\Delta 5/+}$ mice. Generation of *Pten*$^{+/-}$ embryonic stem cells has been described previously (10). The *Pten* exon 5 deletion was generated by transiently transfecting a Cre recombinase–expressing vector into the conditional *Pten* knockout embryonic stem cell line (11) and subsequently selected for thymidine kinase resistant (*tk*^{r}) clones (Supplementary Fig. S1). Two classes of *tk*^{r} embryonic stem clones were generated: (*a*) conditional deletion clones with the exon 5 flanked by loxP sites (*Pten*$^{loxp/+}$; ref. 11) and (*b*) exon 5 deleted clones (*Pten*$^{\Delta 5/+}$). Embryonic stem cell clones carrying either *Pten*$^{+/-}$ or *Pten*$^{\Delta 5/+}$ were injected into either C57/B6 or BALB/c blastocysts. Chimeric male mice were backcrossed to obtain heterozygous mice. F1 mice were then intercrossed for phenotype analysis.

Histology analysis and pathologic grading. Tumors were dissected and fixed in 10% buffered formalin followed by fixation in 70% alcohol. Tumor tissues were paraffin embedded, sectioned (4 μm), and stained with H&E.

PCR and Western blot analysis. To facilitate faster genotyping, a PCR strategy was developed using two primers: forward primer (derived from intron 4 sequence) 5′-ACTCAAGGCAGGGATGAGC-3′ and two reverse primers, P2 (derived from exon 5 sequence) 5′-AATCTAGGGCCT-CTTGTGCC-3′ and P3 (derived from the vector sequence) 5′-GCTTGA-TATCGAATTCCTGCAGC-3′. These primers give rise to the amplified products of 1,100 bp for the loxp allele, 900 bp for the wild-type allele, and 300 bp for the Δ5 allele. To confirm *Pten* deletion, antibodies specific to the NH_2 terminus (Santa Cruz Biotechnology, Santa Cruz, CA) and COOH terminus (Cell Signaling Technologies, Beverly, MA) of the PTEN protein were used.

Note: Supplementary data for this article are available at Cancer Research Online (http://cancerres.aacrjournals.org/).

D. Freeman and R. Lesche contributed equally to this work.

R. Lesche is currently at Epigenomics AG, Kastanienallee 24, 10435 Berlin, Germany.

Requests for reprints: Hong Wu, Department of Molecular and Medical Pharmacology, University of California at Los Angeles School of Medicine, 650 CE Young Drive South, Los Angeles, CA 90095-1735. Phone: 310-825-5160; Fax: 310-267-0242; E-mail: hwu@mednet.ucla.edu.

doi:10.1158/0008-5472.CAN-05-4143

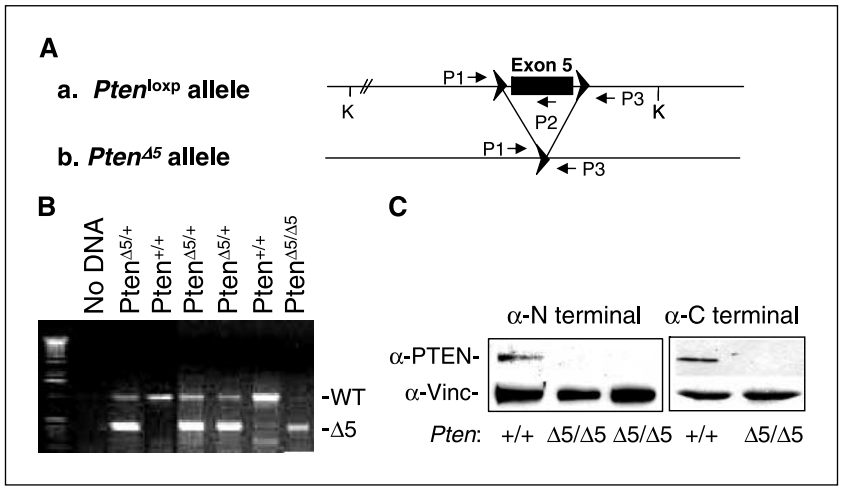

Figure 1. Inactivation of mouse *Pten* gene. *A,* generation of the $Pten^{\Delta 5/+}$ allele. *a,* genomic structure of $Pten^{loxp}$ allele with exon 5 boxed and primers indicated. *b,* $Pten^{\Delta 5/+}$ allele. *B,* PCR analysis of the littermates from $Pten^{\Delta 5/+} \times Pten^{\Delta 5/+}$ crossing. *C,* Western blot analysis of PTEN protein levels in mouse embryonic fibroblast cells derived from injected embryonic stem lines. Cell lysates (20 μg) were run on a polyacrylamide gel and Western blotted with antibodies against the NH_2-terminal (*left*) and COOH-terminal (*right*) of the PTEN protein. The same blots were also reblotted with antivinculin antibody for loading controls.

Results

Generation of $Pten^{\Delta 5/+}$ mice. Embryonic stem cell clones carrying the $Pten^{\Delta 5/+}$ allele were generated by transiently expressing the Cre recombinase in $Pten^{loxp/+}$ embryonic stem cells (ref. 11; Fig. 1*A*). Germ line transmission of the $Pten^{\Delta 5}$ mutant allele was achieved from two independent embryonic stem cell clones. Because the deletion is specific for the exon 5, a PCR screening method was used to determine the mouse genotypes (for primers, see Fig. 1*A*). Intercrosses between heterozygous F1 mice yielded animals of three genotypes: $Pten^{+/+}$, $Pten^{+/\Delta 5}$, and $Pten^{\Delta 5/\Delta 5}$ (Fig. 1*B*). $Pten^{\Delta 5/\Delta 5}$ mice were embryonic lethal and died between embryonic days 9.5 to 10.5 (E9.5-10.5). More detailed morphologic analyses revealed phenotypes that have not been reported by the previous studies (6, 7, 9): mutant embryos exhibit a wavy neural tube (Supplementary Fig. S1, comparing *B* and *D*, areas pointed by *black arrowheads*), failure of neural tube closure (comparing *A* and *C, white arrows*), and pericardial bulging (*A* and *C, black arrows*) at E9.0-9.5, right before the onset of embryonic lethality. No PTEN protein could be detected using either anti-NH_2-terminal or anti-COOH-terminal antibodies (Fig. 1*C*), suggesting that exon 5 deletion leads to either a complete null mutation or a truncated protein that is very unstable.

Onset and spectrum of tumor formation in $Pten^{\Delta 5/+}$ mice. On the 129/BALB/c genetic background, the onset and spectrum of tumor development of $Pten^{\Delta 5/+}$ mice were significantly different from the previous reports, in almost all of which were done on the 129/C57 or 129/CD1 background (Table 1). We have surveyed >150 $Pten^{\Delta 5/+}$ mice, ranging from 1 to 14 months, and did detailed histopathologic analysis on 47 mice, covering tissues and organs, such as brain, thymus, lymph nodes, lung, liver, adrenal glands, pancreas, spleen, uterus, ovary, mammary glands, gastrointestinal tract, and prostate. Our findings can be summarized as follows: (*a*) the onset of tumor formation on the BALB/c background is significantly delayed versus other findings, which report spontaneous development of malignant tumors in <3.5 months (6, 7, 9). The majority of $Pten^{\Delta 5/+}$ heterozygous mice (90%) were tumor free during the first 6 months of their postnatal life, and only 50% of the animals had developed tumors by 10 months of age, as judged

Table 1. *Pten* heterozygous tumor models: a comparison

Features	Pandolfi	Mak	Parsons	Wu
Deletion	Exons 4-5	Exons 3-5	Exon 5	Exon 5
Background	129/C57	129/CD1 or 129/C57	129/C57	129/BALB/c
Homozygotes die at:	<E7.5	E9.5	E6.5	E9.5
Tumors in heterozygotes				
Earliest detection	1.5 mo (6)	2 mo (9)	1.5 mo (7)	6 mo
Tumor types and frequencies				
Gastrointestinal hyperplasia	All? (6)	All? (9)	90% (lymphoid)	2% (inflammation)
Lymphoid hyperplasia	100% female (20) and 83% male (20)	88% (9) (T-cell lymphoma)	100% female and 45% male	33% female and 20% male
Adrenal medullary tumor	100% (21)	23% (8)	NR	None
Endometrial hyperplasia	70% (21)	80% (8)	100%	9% (45% hemangioma)
Breast	NR	49% (8)	NR	37%
Prostate	50% (21)	44% (8)	75%	90%
Thyroid	60% (21)	None (9)	30%	None

Abbreviation: NR, Not reported.

by histologic analysis (12). (*b*) The spectrum of tumors is also quite different (Table 1). Previously reported tumor incidences on the 129/C57 or 129/CD1 backgrounds were biased towards tissues and organs, such as lymphoid, endometrial, adrenal, thyroid, gastrointestinal, and mammary glands (6–9). In our aged animals, ranging from 7 to 14 months, the incidences of lymphoid and endometrial hyperplasia or neoplasia were rather low (25% and 9%, respectively). Heterozygous females were able to produce 6 to 7 litters, and their reproductive life span was similar to wild-type controls. Epithelial hyperplasia/carcinoma of the gastrointestinal tracts and tumors in the adrenal glands were not detected. On the other hand, among 21 male mice analyzed (age, 10-15 months), prostate abnormalities, ranging from hyperplasia to local invasion (Supplementary Fig. S2), were present in 95% heterozygotes. Furthermore, 30% of *Pten*$^{\Delta 5/+}$ female on the 129/BALB/c background also developed mammary tumors, ranging from 1 to 10 tumors per animal, similar to a previous report (ref. 8; Supplementary Fig. S3). In addition, hemangioma lesions were found in 45% of the *Pten*$^{\Delta 5/+}$ female uteri (see below).

Vascular abnormalities in *Pten*$^{\Delta 5/+}$ animals. In addition to hamartomas and increased susceptibility of malignant cancers, patients with inherited *PTEN* mutations also suffer from vascular malformations, such as angiomatosis and hemangiomas (13). Interestingly, vascular lesions, which resemble angiomatosis or hemangiomas, were observed in our *Pten*$^{\Delta 5/+}$ mice. Among 15 females (7-14 months) studied, seven of them had single or multiple solid masses in their uteri horns (Fig. 2*A*). The masses consisted of nonencapsulated aggregates of endothelium-lined, cavernous blood-filled spaces of variable sizes (Fig. 2*B, arrows*). Narrow connective tissue septa separated these vascular spaces. The blood within the larger spaces was often thrombosed (Fig. 2*B, Th*). Occasionally, at the edges of these large cavernous spaces, there were small aggregates of capillaries, whereas in some areas, the tissue resembled arterioles or venules. These smaller vessels always seemed engorged and packed with masses of erythrocytes. These lesions were predominantly in the myometrium, involved the whole uterine wall, and protruded into the uterine lumen.

The vascular abnormalities were also found in the brain (Fig. 2*C* and *D*), mammary glands (Supplementary Fig. S3), spinal cord, and the body walls (data not shown), but with lower frequencies. Figure 2*C* shows a 14-month-old male mouse with vascular lesions in the brain similar to those described in the uterus. This mouse seemed ataxic with enlargement of the forehead. Grossly, the left olfactory bulb and frontal lobes of the cerebrum seemed to be replaced by masses of hemorrhagic-appearing tissue (Fig. 2*D*). Histologically, the mass consisted of aggregates of endothelium-lined, cavernous blood-filled spaces separated by narrow connective tissue septa (Fig. 2*D, white arrow*). The blood within some spaces was thrombosed (Fig. 2*D, Th*) and calcified (Fig. 2*D, Ca*$^{++}$). Small aggregates of capillary arteriole- and venule-like vessels, similar to those seen in the uterus, were also present in the vicinity of the lesion.

Although most lesions were benign and isolated, malignant transformation was observed in three cases: two with local invasion and one with whole body metastasis. Figure 2*E* shows an example of liver metastasis. Similar lesions were also observed in the spleen, lymph nodes, intestine, lung, and many other organs in the same animal. Sectioning through the metastatic lesion in the liver reveals cord-like epithelial engulfing masses of erythrocytes. Thus, similar to what has been reported in humans, PTEN also controls vascular morphogenesis and possibly vascular functions in our knockout models.

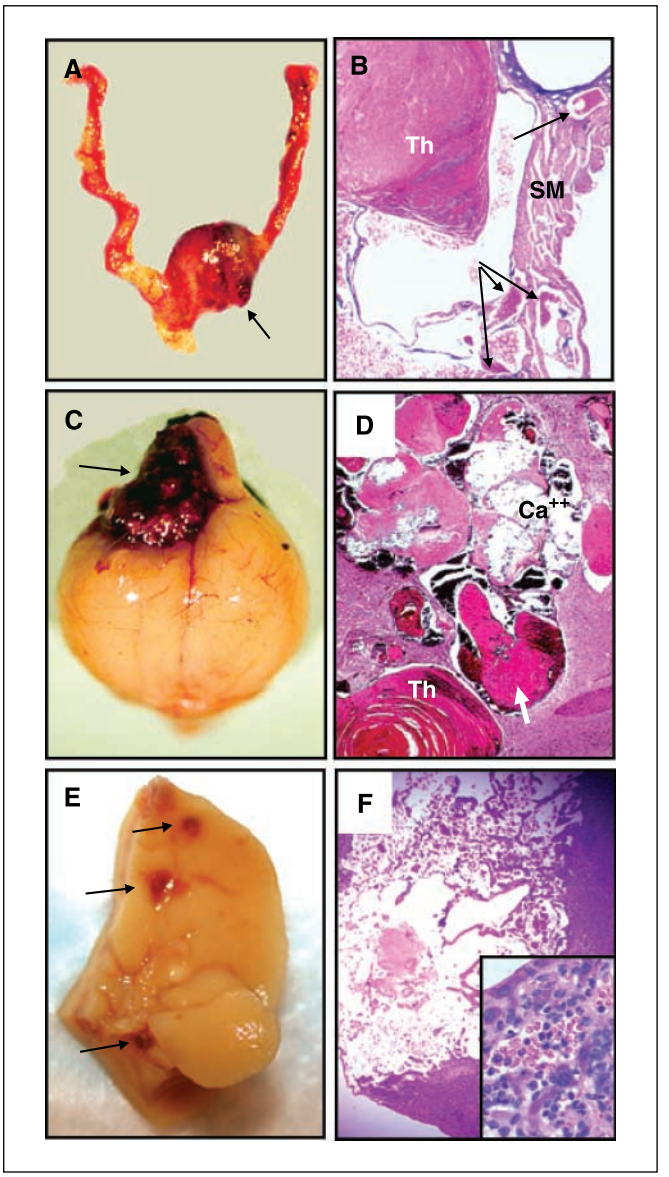

Figure 2. Hemangiomas in *Pten*$^{\Delta 5/+}$ mice. *A, C*, and *E*, gross appearances of vascular lesions in different mutant animals. *B, D*, and *F*, histologic features of the corresponding lesions on the left. Arrows in (*B*) indicate endothelium-lined vascular space with one contains a thrombus (*Th*). *D*, vascular lesion in the brain of a *Pten*$^{\Delta 5/+}$ mouse. Large cavernous endothelium-lined spaces filled with thrombotic blood and foci of calcification (*Ca*$^{++}$). *F*, metastatic lesions in the liver. Photos were taken with ×4 (*B, D*, and *F*) and ×40 (*F, inset*) objective lens. Bar, 200 mm (*B, D*, and *F*).

Genetic background influences tumor development. Such phenotypic differences could be due to (*a*) hypomorphic properties of specific mutations created by individual research groups or (*b*) the influence of genetic background or modifier gene(s). To distinguish between these two possibilities, we compared the exon 5–specific deleted mouse strain with another heterozygous *Pten* knockout mouse strain generated in our laboratory, in which both transcriptional and translational start sites and exons 1 to 3 of the *Pten* gene were deleted (*Pten*$^{+/-}$; ref. 10). In the postnatal 7 months, the onset and spectrum of tumor development of *Pten*$^{+/-}$ mice on BALB/c/129 background is similar to *Pten*$^{\Delta 5/+}$ mice but differ

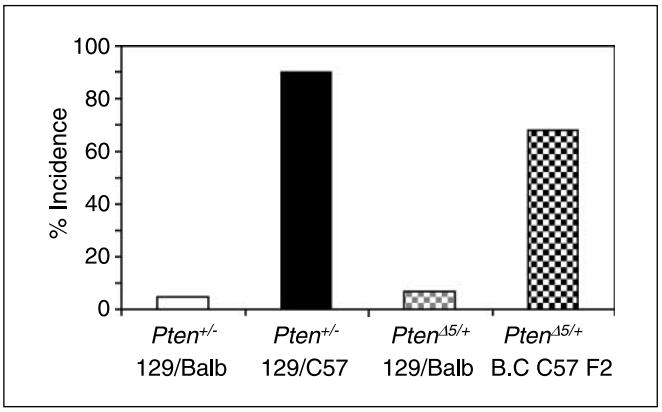

Figure 3. Incidences of lymphoma formation in $Pten^{+/-}$ and $Pten^{\Delta 5/+}$ mice depend on genetic background. Percentages of animals that develop lymphoma within 1 to 7 months are illustrated. 129/BALB and 129/C57: animals from 129/BALB or 129/C57 F1 intercrossing. B.C C57 F2: $Pten^{\Delta 5/+}$ mice were backcrossed to C57 mice, and their F2 offspring were analyzed.

significantly to itself on C57/129 background (Fig. 3, *columns 1* and *2*). Interestingly, the tumor phenotypes observed in $Pten^{+/-}$ mice on C57/129 background are very close to published reports (Table 1). Similarly, when we backcrossed BALB/c/129 $Pten^{\Delta 5/+}$ mice to C57/BL6 background, we found that 85% of $Pten^{\Delta 5/+}$ F2 female mice developed lymphoid hyperplasia and 56% with cystic endometrial hyperplasia (comparing to 25% and 9%, respectively, on the 129/BALB/c background). Furthermore, the onset of such abnormalities developed much earlier: 70% F2 heterozygous females developed lymphoid hyperplasia between 1 and 7 months compared with only 10% found in 129/BALB/c heterozygous females at similar age (Fig. 3, *columns 3* and *4*). This genetic study indicates that genetic background or modifier gene(s) play an important role in regulating PTEN's *in vivo* functions.

Discussion

This study as well as other published studies observed increased tumor formation in animals harboring heterozygous mutations of *Pten*. However, tumor frequency, tumor spectrum, and onset of the tumors varied significantly. Multiple factors could contribute to the observed phenotypic differences. Although all published mutations were generated around exon 5 of the *Pten* gene, each group has employed slightly different strategies to create their specific mutation. Whether these different mutations code for truncated proteins that may display various hypomorphic or dominant-negative properties is currently unknown. In this study, we have directly compared two independent mutations in the murine *Pten* locus: one carries deletion from the promoter through exon 3, thus should be completely null (10), and the other with exon 5–specific deletion (this study). Biochemical analysis showed that no protein products could be detected from either type of mutations, suggesting that if a truncated protein is produced from either one of the deletion mutations, it must be very unstable. Furthermore, analyzing the onset and spectrum of tumor formation indicated that the major contributor to the phenotype variation was the genetic background, not the particular mutation generated.

Although, to date, vascular abnormalities in $Pten^{\Delta 5/+}$ animals on the 129/BALB/c background have not been reported, recent studies suggest that PTEN/phosphatidylinositol 3-kinase pathway controls normal vascular development and tumor angiogenesis (14–17), and AKT-1, the downstream effector of PTEN, regulates pathologic angiogenesis, vascular maturation, and permeability *in vivo* (18). Thus, the *Pten* knockout mice generated in this study may facilitate our understanding of PTEN-controlled angiogenesis *in vivo*.

Our finding that the genetic background or modifier gene(s) may play an essential role in modulating PTEN's biological functions is both biologically relevant and clinically significant. Strain-dependent phenotypes and modifying loci in tumorigenesis have been well documented in mouse models, such as the *Mom-1* locus for intestinal polyposis syndromes in $Min^{+/-}$ mice (19). The significant differences of the observed phenotypes on two different genetic backgrounds correspond well with the striking differences seen in the human familial disorders with reported *PTEN* mutations. At least two possibilities could account for this observation: (*a*) differences in the rate of *PTEN* loss or loss of heterozygosity, which is inherited by individual patient or mouse strain and (*b*) allelic differences in other disease-modifying genes that have not yet been identified. Further detailed genetic analysis and comparisons of the different *Pten* mutant mice will be valuable to uncover additional information in our understanding of PTEN's *in vivo* function and genotype/phenotype relationship.

Acknowledgments

Received 11/18/2005; revised 3/23/2006; accepted 5/1/2006.

Grant support: NIH grants CA98013 (H. Wu), Department of Defense grants PC991538 (H. Wu), Prostate Cancer Foundation (H. Wu), Howard Hughes Medical Institute (R. Lesche), Deutsche Forschungsgemeinschaft (R. Lesche), and Predoctoral Research Training Grant in Pharmacological Sciences and Prostate Cancer Foundation (D. Freeman).

The costs of publication of this article were defrayed in part by the payment of page charges. This article must therefore be hereby marked *advertisement* in accordance with 18 U.S.C. Section 1734 solely to indicate this fact.

We thank members of our laboratories for helpful comments, Dr. Robert D. Cardiff for pathologic evaluation and immunohistochemistry analysis, and Margy Blavin for article preparation.

References

1. Li DM, Sun H. TEP1, encoded by a candidate tumor suppressor locus, is a novel protein tyrosine phosphatase regulated by transforming growth factor beta. Cancer Res 1997;57:2124–9.
2. Steck PA, Pershouse MA, Jasser SA, et al. Identification of a candidate tumour suppressor gene, MMAC1, at chromosome 10q23.3 that is mutated in multiple advanced cancers. Nat Genet 1997;15:356–62.
3. Liaw D, Marsh DJ, Li J, et al. Germline mutations of the PTEN gene in Cowden disease, an inherited breast and thyroid cancer syndrome. Nat Genet 1997;16:64–7.
4. Nelen MR, van Staveren WC, Peeters EA, et al. Germline mutations in the PTEN/MMAC1 gene in patients with Cowden disease. Hum Mol Genet 1997;6:1383–7.
5. Marsh DJ, Kum JB, Lunetta KL, et al. PTEN mutation spectrum and genotype-phenotype correlations in Bannayan- Riley-Ruvalcaba syndrome suggest a single entity with Cowden syndrome. Hum Mol Genet 1999;8:1461–72.
6. Di Cristofano A, Pesce B, Cordon-Cardo C, Pandolfi PP. Pten is essential for embryonic development and tumour suppression. Nat Genet 1998;19:348–55.
7. Podsypanina K, Ellenson LH, Nemes A, et al. Mutation of Pten/Mmac1 in mice causes neoplasia in multiple organ systems. Proc Natl Acad Sci U S A 1999;96:1563–8.
8. Stambolic V, Tsao MS, Macpherson D, et al. High incidence of breast and endometrial neoplasia resembling human Cowden syndrome in $pten^{+/-}$ mice. Cancer Res 2000;60:3605–11.
9. Suzuki A, de la Pompa JL, Stambolic V, et al. High cancer susceptibility and embryonic lethality associated with mutation of the PTEN tumor suppressor gene in mice. Curr Biol 1998;8:1169–78.
10. Sun H, Lesche R, Li DM, et al. PTEN modulates cell cycle progression and cell survival by regulating

phosphatidylinositol 3,4,5,-trisphosphate and Akt/protein kinase B signaling pathway. Proc Natl Acad Sci U S A 1999;96:6199–204.
11. Lesche R, Groszer M, Gao J, et al. Genesis 2002;32:148–9.
12. Freeman DJ, Li AG, Wei G, et al. PTEN tumor suppressor regulates p53 protein levels and activity through phosphatase-dependent and -independent mechanisms. Cancer Cell 2003;3:117–30.
13. Zonana J, Rimoin DL, Davis DC. Macrocephaly with multiple lipomas and hemangiomas. J Pediatr 1976;89:600–3.
14. Jiang BH, Zheng JZ, Aoki M, Vogt PK. Phosphatidylinositol 3-kinase signaling mediates angiogenesis and expression of vascular endothelial growth factor in endothelial cells. Proc Natl Acad Sci U S A 2000;97:1749–53.
15. Wen S, Stolarov J, Myers MP, et al. PTEN controls tumor-induced angiogenesis. Proc Natl Acad Sci U S A 2001;98:4622–7.
16. Zhong H, Chiles K, Feldser D, et al. Modulation of hypoxia-inducible factor 1alpha expression by the epidermal growth factor/phosphatidylinositol 3-kinase/PTEN/AKT/FRAP pathway in human prostate cancer cells: implications for tumor angiogenesis and therapeutics. Cancer Res 2000;60:1541–5.
17. Hamada K, Sasaki T, Koni PA, et al. The PTEN/PI3K pathway governs normal vascular development and tumor angiogenesis. Genes Dev 2005;19:2054–65.
18. Chen J, Somanath PR, Razorenova O, et al. Akt1 regulates pathological angiogenesis, vascular maturation and permeability *in vivo*. Nat Med 2005;11:1188–96.
19. Dietrich WF, Lander ES, Smith JS, et al. Genetic identification of Mom-1, a major modifier locus affecting Min-induced intestinal neoplasia in the mouse. Cell 1993;75:631–9.
20. Di Cristofano A, Kotsi P, Peng YF, Cordon-Cardo C, Elkon KB, Pandolfi PP. Impaired Fas response and autoimmunity in $Pten^{+/-}$ mice. Science 1999;285:2122–5.
21. Di Cristofano A, De Acetis M, Koff A, Cordon-Cardo C, Pandolfi PP. Pten and p27KIP1 cooperate in prostate cancer tumor suppression in the mouse. Nat Genet 2001;27:222–4.